JOURNAL OF PURE AND APPLIED MICROBIOLOGY, Nov. 2013. Vol. 7(Spl. Edn.), p. 333-339

Preparation and Characterization of Nano-magnetic $Ni_{0.5}Mg_{0.5}Fe_2O_4$ System for Biological Applications

N.M. Deraz[1]* and Omar H. Abd-Elkader[2,3]

[1]Physical Chemistry Department, Laboratory of Surface Chemistry and Catalysis, National Research Center, Dokki, Cairo, Egypt.
[2]Zoology Department, College of Science, King Saud University, Riyadh - 11451, Kingdom of Saudi Arabia.
[3]Electron Microscope and Thin Films Department, National Research Center (NRC), El- Behooth Street - 12622, Giza.

(Received: 26 August 2013; accepted: 31 October 2013)

New route was used for preparation of mixed nickel-magnesium ferrite ($Ni_{0.5}Mg_{0.5}Fe_2O_4$). Various techniques were used to characterize the as prepared product such as X-ray diffraction (XRD), infrared (IR) spectroscopy, scanning electron micrographs (SEM), energy dispersive X-ray (EDX) and a vibrating sample magnetometer (VSM). The crystallite size, lattice constant, unit cell volume, density of $Ni_{0.5}Mg_{0.5}Fe_2O_4$ phase has been determined. The investigated method led to prepare single phase of spinel nickel-magnesium ferrite depending upon the XRD and IR results. SEM and EDX techniques showed the as synthesized materials were spongy, homogeneous and fragile. The concentrations of O, Ni, Fe and Mg species involved in $Ni_{0.5}Mg_{0.5}Fe_2O_4$ sample were investigated from the uppermost surface to the bulk layers. The saturation magnetization (Ms), remanence magnetization (Mr) and coercivity (Hc) of the as synthesized composite were 34 emu/g, 12 emu/g and 29 Oe, respectively.

Key words: XRD, SEM, EDX, $Ni_{0.5}Mg_{0.5}Fe_{2O4}$, Crystallite size.

Spinel ferrite based nanostructured materials have received considerable attention from scientists depending upon the broad practical applications in different fields such as surface chemistry and catalysis, sensors and magnetic technologies[1-6]. Magnetic oxide nano-particles with proper surface coatings are increasingly being evaluated for clinical applications such as hyperthermia, drug delivery, magnetic resonance imaging, transfection and cell/protein separations. Applications of these materials could be attributed to unusual physical and chemical properties of ferrite materials. Among these materials, nickel ferrite ($NiFe_2O_4$) and magnesium ferrite ($MgFe_2O_4$) are one of the most important spinel ferrites.

* To whom all correspondence should be addressed.
E-mail: nmderaz@yahoo.com

In fact, nickel ferrite has high magneto crystalline anisotropy, high saturation magnetization and unique magnetic structure[7]. So, the spinel $NiFe_2O_4$ displays various types of magnetic properties such as paramagnetic, superparamagnetic or ferrimagnetic behavior depending on the microstructure[8]. From our previous investigation, glycine assisted combustion method resulted in formation of nickel ferrite with high desulfurization behaviour[1]. Removal of sulphur from commercial kerosene increases as the formation of nickel ferrite increases. However, room temperature magnetization results showed a ferromagnetic behaviour of the $NiFe_2O_4$ nanoparticles, with magnetization and corecivities values in the range of 2.387- 57 emu/g and 65.58 - 148.8 Oe at 15 kOe according to the change in the ratio between glycine and metal nitrates[2]. Depending upon the combustion route, magnesium ferrite has been prepared[3].

The preparation methodology of the ferrite materials, such as Ni- and Mg- ferrites, is influenced by their composition, purity and microstructure. However, the conventionally method to prepare the most ceramic materials can be achieved by the solid state reaction technique. But, this technique has some disadvantages such as elevated preparation temperatures, no homogeneity of the product, poor stoichiometry, and larger crystallite size of the ceramic solids[9, 10].In addition, various methods were used for preparation of different ferrites[11, 12]. Among the preparation methods ferrite materials, the combustion route is one of the abundantly used methods. This method does not require extremely high processing temperatures, expensive materials, high reaction temperatures, long reaction time and toxic. Also, the combustion method resulted in formation of stoichiometric and nanosized materials with high purity[1-3]. The use of glycine in the combustion process be better than other types of fuel as a result of the large negative heat of combustion[13].

This study is focused on preparation of nano-crystalline $Ni_{0.5}Mg_{0.5}Fe_2O_4$ by glycine - assisted combustion route. In addition, the structural, morphological and magnetic properties of this ferrite have been determined. Various techniques were used for characterization of the as synthesized system.

EXPERIMENTAL

Preparation procedure

Nano- particles of $Ni_{0.5}Mg_{0.5}Fe_2O_4$ sample was prepared by mixing calculated proportions of nickel, magnesium and iron nitrates with glycine as fuel. The mixed precursors were concentrated in a porcelain crucible on a hot plate at 400 °C for 5 minutes. The crystal water was gradually vaporized during heating and when a crucible temperature was reached, a great deal of foams produced and spark appeared at one corner which spread through the mass, yielding a brown voluminous and fluffy product in the container. In our experiment, the ratio of the H_2NCH_2COOH : $Ni(NO_3)_2.4H_2O$: $Mg(NO_3)_2.6H_2O$: $Fe(NO_3)_3.9H_2O$ were 4 : 0.5 : 0.5 : 2, respectively. The chemicals employed in the present work were of analytical grade supplied by Prolabo Company.

Characterization technique

An X-ray measurement of various mixed solids was carried out using a BRUKER D8 advance diffractometer (Germany). The patterns were run with Cu K radiation at 40 kV and 40 mA with scanning speed in 2 of 2 ° min^{-1}.

The crystallite size of $Ni_{0.5}Mg_{0.5}Fe_2O_4$ present in the investigated solids was based on X-ray diffraction line broadening and calculated by using Scherrer equation[14].

$$d = \frac{B\lambda}{\beta \cos\theta} \quad ...(1)$$

where d is the average crystallite size of the phase under investigation, B is the Scherrer constant (0.89), λ is the wave length of X-ray beam used, is the full-width half maximum (FWHM) of diffraction and is the Bragg's angle.

An infrared transmission spectrum of various solids was determined using Perkin-Elmer Spectrophotometer (type 1430). The IR spectra were determined from 900 to 300 cm^{-1}. Two mg of each solid sample were mixed with 200 mg of vacuum-dried IR-grade KBr. The mixture was dispersed by grinding for 3 min in a vibratory ball mill and placed in a steel die 13 mm in diameter and subjected to a pressure of 12 tones. The sample disks were placed in the holder of the double grating IR spectrometer.

Table 1. The atomic abundance of elements measured at 20 keV and different points over the as prepared sample.

Sample	Elements	Point 1	Point 2	Point 3
	O	10.84	11.34	12.10
Ni-Mg	Mg	1.61	1.78	1.73
ferrite	Fe	73.60	72.19	72.07
	Ni	13.95	14.69	14.10

Table 2. The atomic abundance of elements measured at different applied voltages on the one point over the as prepared sample.

Sample	Elements	10keV	15keV	20keV
	O	30.55	18.21	6.22
Ni-Mg	Mg	4.81	2.54	1.09
ferrite	Fe	57.33	66.73	79.12
	Ni	7.31	12.52	13.57

Scanning electron micrographs (SEM) was recorded on JEOL JAX-840A electron micro-analyzer. The sample was dispersed in ethanol and then treated ultrasonically in order to disperse individual particles over gold grids.

Energy dispersive X-ray analysis (EDX) was carried out on Hitachi S-800 electron microscope with an attached kevex Delta system. The parameters were as follows: accelerating voltage 15 keV, accumulation time 100s, window width 8 µm. The surface molar composition was determined by the Asa method, Zaf-correction, Gaussian approximation.

The magnetic properties of the investigated solids were measured at room temperature using a vibrating sample magnetometer (VSM; 9600^{-1} LDJ, USA) in a maximum applied field of 15 kOe. From the obtained hysteresis loops, the saturation magnetization (Ms), remanence magnetization (Mr) and coercivity (Hc) were determined.

RESULTS

XRD Investigation

X- ray diffractograms of the as prepared sample are illustrated in Fig. 1. The as synthesized specimen consisted entirely of nano-crystalline spinel $Ni_{0.5}Mg_{0.5}Fe_2O_4$ phase with the Fd3m space group (JCPDS card No. 80-0072). The crystal planes of the $Ni_{0.5}Mg_{0.5}Fe_2O_4$ spinel are (1 1 1), (2 2 0), (311), (2 2 2), (4 0 0), (4 2 2), (5 1 1), (4 4 0), (5 3 3), (6 2 2), (4 4 4) and (6 4 2) respectively. The average crystallite size of $Ni_{0.5}Mg_{0.5}Fe_2O_4$ phase was

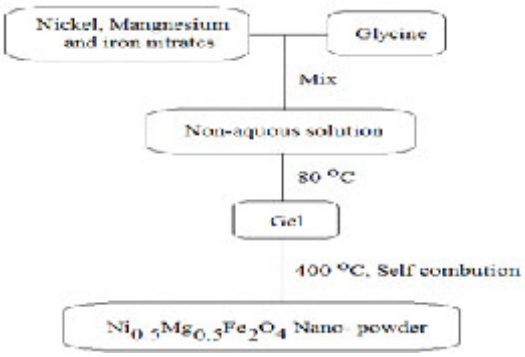

Fig. 1. Process flowchart for fabricating $Ni_{0.5}Mg_{0.5}Fe_2O_4$ sample

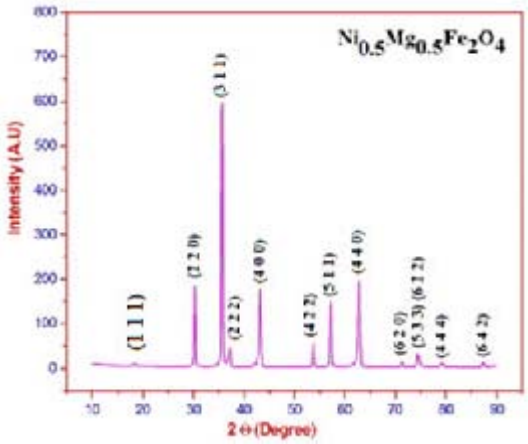

Fig. 2. XRD pattern for Ni-Mg ferrite sample

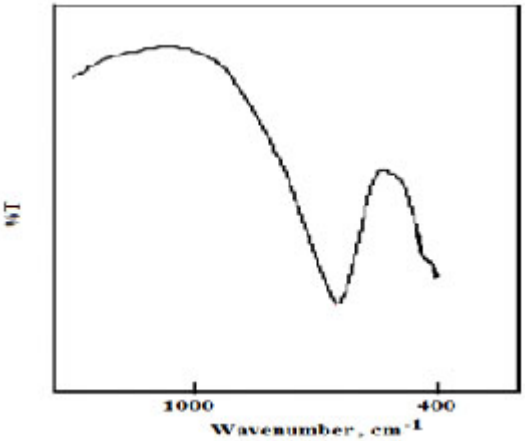

Fig. 3. IR spectra for Ni-Mg ferrite sample with different magnifications

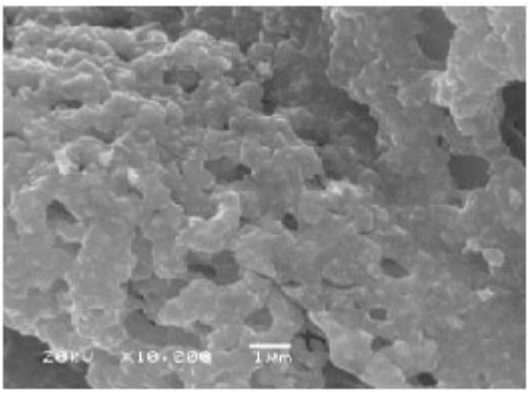

Fig. 4. SEM images for Ni-Mg ferrite sample

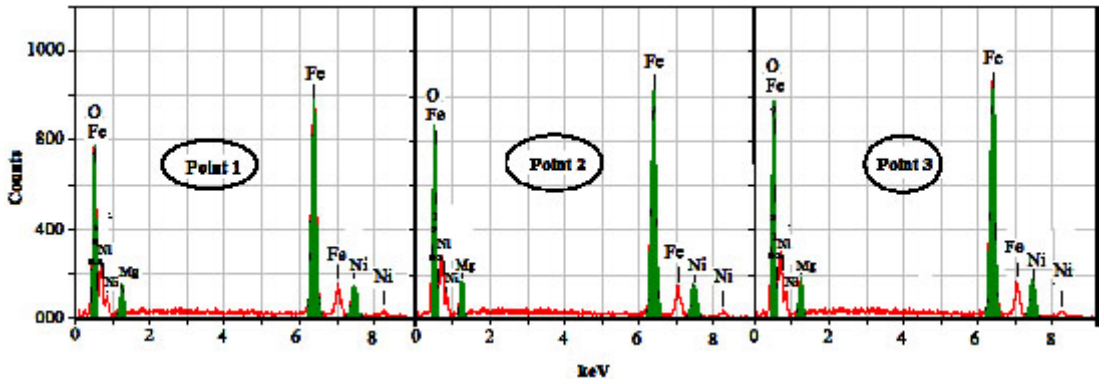

Fig. 5. EDX pattern $Ni_{0.5}Mg_{0.5}Fe_2O_4$ sample with different points

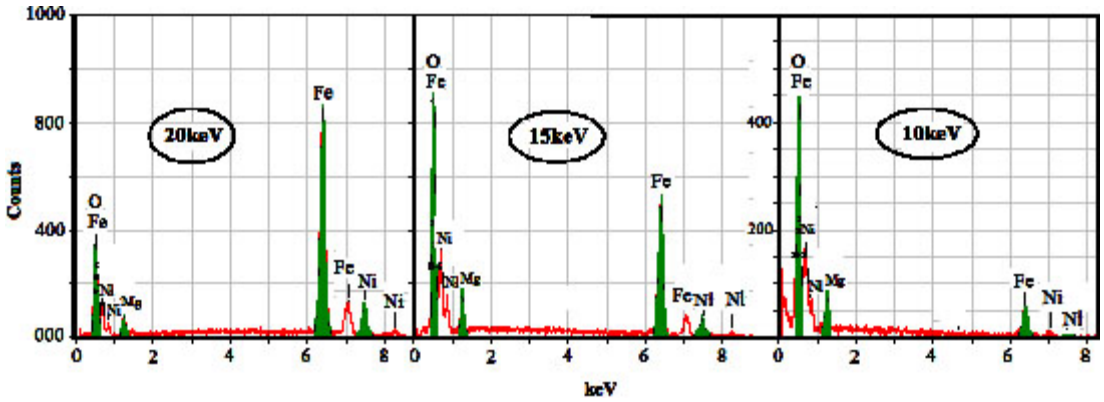

Fig. 6. EDX pattern of $Ni_{0.5}Mg_{0.5}Fe_2O_4$ sample with different voltages

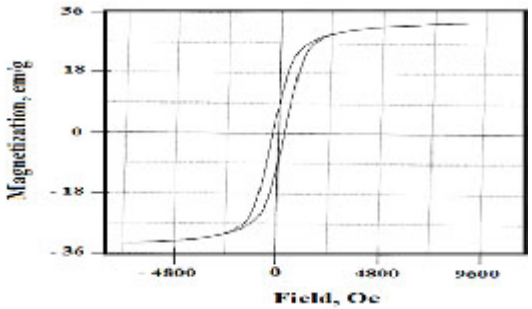

Fig. 7. Magnetic hysteresis curves measured at a room temperature for the as prepared sample

estimated to be about 50 nm. The as prepared ferrite consisted of single spinel $Ni_{0.5}Mg_{0.5}Fe_2O_4$ phase depending upon absence of any additional peak related to any second phase.

X-ray data enable us to determine the different structural parameters as the lattice constant (a), unit cell volume (V), X-ray density (Dx), the distance between the magnetic ions (L_A and L_B), ionic radii (r_A, r_B) and bond lengths (A-O and B-O) on tetrahedral (A) sites and octahedral (B) sites of $Ni_{0.5}Mg_{0.5}Fe_2O_4$ crystallites. The estimated values of a, LA, LB , rA, rB, A-O and B-O of $Ni_{0.5}Mg_{0.5}Fe_2O_4$ particles are 0.8340, 0.3511, 1.1684, 0.0680, 0.0672, 0.1923 and 0.2021 nm, respectively. Whereas, the value of V is 0.5809 nm^3 while the value of Dx is 4.9651 g/cm^3.

IR analysis

IR spectra of the as prepared ferrites ranged from 1000 to 400 cm^{-1} are shown in Fig. 3. Spinel ferrites have two main metal- oxygen bands in IR pattern[19]. These bands indicate the tetrahedral (A-sites) and octahedral (B-sites) involved in the spinel structure according to the geometrical configuration of materials. The highest band υ_1, locates around 600 cm^{-1}, corresponds to intrinsic stretching vibrations of metal at the tetrahedral site, whereas the υ_2 lowest band, appears around 400 cm^{-1}, is assigned to octahedral- metal stretching. In this study, there are two bands, υ_1 and υ_2, at 649 and 445 cm^{-1}, respectively, indicating to the presence of spinel Ni-Mg ferrite.

SEM investigation

The morphology of the as synthesized sample can be investigated by scanning electron micrographs (SEM) as shown in Fig. 4.

It can be seen from this figure that the glycine - assisted combustion method resulted in polyhedron, spongy and fragile material containing voids and pores. These observations could be attributed to the release of large amounts of gases during combustion process depending upon decomposition of both glycine and metals nitrate.

EDX measurements

Energy dispersive X-ray (EDX) analysis with different voltages and also different points on the surface of sample has been investigated. Fig. 5 shows EDX spectrum at different points on the surface of sample to determine the homogeneity of the investigated sample. Fig. 6 displays EDX pattern at the one point on the surface of sample with different applied voltages to determine the gradient of elements involved in the sample studied.

Homogeneity of elements

Table 2 shows the concentrations of different constituents involved in the investigated sample at 20 keV over different points on the solid surface. This table indicates that the concentrations of different constituents (O, Mg, Fe and Ni) are very close to each other. This confirms the homogeneity of the as prepared system.

The element gradient

The concentrations of O, Mg, Fe and Ni species from the uppermost surface to the bulk layers of the sample of Ni-Mg ferrite can be calculated using EDX technique at 10, 15 and 20 keV as shown in Table 2. This table showed that the surface concentrations of Mg and O species for the as prepared sample decrease as the applied voltage increases. The opposite behavior was observed in the case of both Ni and Fe species.

Magnetic properties

The magnetic hysteresis loop at room temperature of the as-prepared powders resulted in determination of their magnetic properties as shown in Fig. 7. The values of Ms, Mr and Hc for the as prepared sample were 34 emu/g, 12 emu/g and 29 Oe, respectively. From our previous studies, it was found that the magnetization of the as prepared sample is larger than that of $MgFe_2O_4$[3]. Opposite behavior was observed in the case of $NiFe_2O_4$[2].

DISCUSSION

In this study, new method was used for mixed ferrites such as $Ni_{0.5}Mg_{0.5}Fe_2O_4$ nano-particles. This method is glycine- assisted combustion route. Our research group was used this method for preparation different ceramic materials especially the simple ferrite such as $NiFe_2O_4$, $MgFe_2O_4$ and so on[1-3]. This depends upon the environmental benignity, high yield, inexpensive and high safety of this method. In addition, this route is a simple one-step and "green" strategy for the synthesis of various ferrites.

The diffusion of Mg^{2+}, Ni^{2+} and Fe^{3+} through early rigid ferrite film led to the formation of $Ni_{0.5}Mg_{0.5}Fe_2O_4$particles[1-3]. The diffusing ions might be Fe^{2+} including Fe^{3+} depending on the detecting Fe^{2+} in the interface[15]. Some authors indicate that Fe_2O_3 decomposes to $2Fe^{2+}$ and oxygen gas at Fe_2O_3-interface[16]. Moreover, oxygen moves through the reacted area to be added to the NiO and Mg O interfaces in order to form spinel by reacting with Fe^{2+} and NiO and MgO:

At Fe_2O_3 interface

$$3Fe_2O_3 + Ni^{2+} + Mg^{2+} \rightarrow 2Ni_{0.5}Mg_{0.5}Fe_2O_4 + 2Fe^{2+} + 0.5O_2 \quad ...(2)$$

At NiO and MgO interfaces

$$2Fe^{2+} + 1.5NiO + 1.5\,MgO + 0.5O_2 \rightarrow Ni_{0.5}Mg_{0.5}Fe_2O_4 + Ni^{2+} + Mg^{2+} \quad ...(3)$$

The difference in the ionic radii of ferric, nickel and magnesium species are 0.064, 0.078 and 0.065 nm, respectively, brought about the diffusion of the reacting cations with subsequent chemically created vacancies[1-3]. In fact, EDX measurements showed the surface concentrations of O species decreases as the applied voltage increases. This suggests to create the chemically vacancies. Depending upon the electro-neutrality restrictions, formation of $2Fe^{3+}$ and a vacancy is due to the replacement of Ni^{2+} or Mg^{2+}. An embryonic element or nucleus for formation of spinel in order to satisfy energy stabilization in the structure is the introduction of trivalent cations into NiO or MgO with appearance of ferric cations in tetrahedral sites involved in the spinel structure [17]. The strong bond between Fe^{3+} cations with O^{2-} ions at tetrahedral

site due to an electro-negativity differences resulted in the lowest state of energy[17].

The comparison between the structural parameters (especially a, V and Dx) for $Ni_{0.5}Mg_{0.5}Fe_2O_4$ system in this study and both $NiFe_2O_4$ and $MgFe_2O_4$ systems in our previous researchs is very important. Indeed, the values of different sturactural parameters are in the range between that for both $NiFe_2O_4$ and $MgFe_2O_4$ systems. These findings confirm that the investgated product is between these ferrites. This evidence supported by the shift in the d-spacing of $Ni_{0.5}Mg_{0.5}Fe_2O_4$ relative to that of both $NiFe_2O_4$ and $MgFe_2O_4$ systems depening upon the XRD data.The lattice parameter of $Ni_{0.5}Mg_{0.5}Fe_2O_4$ was found to be 0.8340 nm, which is in agreement with the reported values of 0.8340 nm and 0.8368 for $NiFe_2O_4$ and $MgFe_2O_4$, respectively[3]. It is possible to distinguish $Ni_{0.5}Mg_{0.5}Fe_2O_4$ by XRD technique depending upon the change of the lattice parameter of both $NiFe_2O_4$ and $MgFe_2O_4$ between the values 0.8380 - 0.840 nm[18]. However, IR measurement confirms the formation of $Ni_{0.5}Mg_{0.5}Fe_2O_4$ spinel.

EDX measurements showed that the surface concentrations of Ni and Fe species for the as prepared sample increase and that of Mg and O decrease as the applied voltage increases. This indicates that MgO was dissolved in both NiO and Fe_2O_3 solids forming $Ni_{0.5}Mg_{0.5}Fe_2O_4$ solid.

SEM and EDX measurements showed that the investigated method led to formation of fragile, spongy and homogeneous Ni0.5Mg0.5 Fe_2O_4 solid as a single phase. In other words, the glycine assited combusion method led to formation of fine, foamy and voluminous Ni-Mg ferrite[20]. The results of XRD confirm the formation of single spinel $Ni_{0.5}Mg_{0.5}Fe_2O_4$ phase.

There are difference between the magnetization of the as synthesized $Ni_{0.5}Mg_{0.5}Fe_2O_4$ sample and that of both Ni and Mg ferrites prepared by the same method in our previous investigations[2, 3]. This can be attributed to difference between the magnetic moments of Mg ions and that for Ni ions and/or the exchange-coupling interaction in the $Ni_{0.5}Mg_{0.5}Fe_2O_4$ sample[21].

CONCLUSIONS

Solid state reaction between NiO, MgO and Fe_2O_3 led to formation of Ni-Mg ferrite by using various methods. One of these methods is glycine-assisted combustion method. This route resulted in formation spinel $Ni_{0.5}Mg_{0.5}Fe_2O_4$ system depending upon XRD and IR data. The crystallite size, lattice constant and unit cell volume of $Ni_{0.5}Mg_{0.5}Fe_2O_4$ system display formation of nano-crystalline $Ni_{0.5}Mg_{0.5}Fe_2O_4$ as single phase. However, the liberation of different gases during preparation process brought about spongy and homogeneous material as shown in the SEM and EDX measurements. The values of Ms, Mr and Hc for $Ni_{0.5}Mg_{0.5}Fe_2O_4$ system were 34 emu/g, 12 emu/g and 29 Oe, respectively.

ACKNOWLEDGMENTS

The authors would like to extend their sincere appreciation to the Deanship of Scientific Research at King Saud University for its funding of this research through the Research Group Project no. RGP- VPP- 306.

REFERENCES

1. Deraz N.M.; Alarifi A.; Shaban S.A.; Removal of sulfur from commercial kerosene using nanocrystalline $NiFe_2O_4$ based sorbents, *J. Saud. Chem. Soc*. 2010; **14**: 357-362.
2. Alarifi A.; Deraz N.M.; Shaban S.A.; Structural, morphological and magnetic properties of $NiFe_2O_4$ nanoparticles, *J. Alloys Compds*. 2009; **486**: 501-506.
3. Deraz N.M.; Alarifi A.; Novel preparation and properties of magnesioferrite nanoparticles, *J. Anal. Appl. Pyrolysis* 2012; **97**: 55-61.
4. Yue W.; Changhong S.; Wei Y.; Fabrication and magnetic properties of $NiFe_2O_4$ nanorods, *Rare Metals* 2010; **29**: 385-389.
5. Raj K., Moskowitz B., Casciari R., Advances in ferrofluid technology, *J. Magn. Magn. Mater.*,1995; **149**: 174-180.
6. Wang J.; Zhua Y.J.; Lia W.P.; Chen Q.W.; Necklace-shaped assembly of single-crystal $NiFe_2O_4$ nanospheres under magnetic field, *Mater. Lett*. 2005; **59**: 2101-2103.
7. Speliotis D.E.; Magnetic recording beyond the first 100 years, *J. Magn. Magn. Mater*. 1999; **193**: 29-35.
8. Younas M.; Nadeem M.; Atif M.; Grossinger R., Metal-semiconductor transition in $NiFe_2O_4$ nanoparticles due to reverse cationic distribution by impedance spectroscopy, *J. Appl. Phys*. 2011; **109**: 093704-093711.

9. Deraz N.M.; Hessien M.M.; Structural and magnetic properties of pure and doped nanocrystalline cadmium ferrite, *J. Alloys Compds.* 2009; **475**: 832-839.
10. Deraz N.M.; Production and characterization of pure and doped copper ferrite nanoparticles, *J. Anal. Appl. Pyrolysis* 2008; **82**: 212-222.
11. Niasari M.S.; Davar F., Mahmoudi T.; A simple route to synthesize nanocrystalline nickel ferrite (NiFe2O4) in the presence of octanoic acid as a surfactant, *Polyhedron* 2009; **28**: 1455-1458.
12. Naseri M.G.; Saion E.B.; Ahangar H.A.; Hashim M.; Shaari A.H.; Simple preparation and characterization of nickel ferrite nanocrystals by a thermal treatment method, *Powder Technol*. 2011; **212**: 80-88.
13. Hwang C.C.; Tsai J.S.; Huang T.H.; Combustion synthesis of Ni-Zn ferrite by using glycine and metal nitrates-investigations of precursor homogeneity, product reproducibility, and reaction mechanism, *Mater. Chem. Phys*. 2005; **93**: 330-336.
14. Cullity B. D.; Elements of X-ray Diffraction; Addison-Wesly Publishing Co. Inc. 1976 (Chapter 14).
15. Alper, High Temperature Oxides, Academic Press, New York, 1970.
16. A. Azhari, Sharif Sh M.; Golestanifard F.; Saberi A., Phase evolution in Fe_2O_3/MgO nanocomposite prepared via a simple precipitation method, *Mater. Chem. Physics* 2010; **124**: 658-663.
17. Blank S.L., Pask J.A., Diffusion of iron and nickel in magnesium oxide single crystals, *J. Am. Ceram. Soc*. 1969; **52**: 669-675.
18. Allen G. C.; Jutson J.A.; Tempest P.A.; Characterization of nickel- chromium iron spinel-type oxides, *J. Nucl. Mater.* 1988, **158**: 96-107.
19. Waldron R. D., Infrared Spectra of Ferrites, *Phys. Rev*. 1955; **99**: 1727.
20. Patil K. C., Hegde M. S., Rattan T., Aruna S. T., Chemistry of nanocrystalline oxide materials combustion Synthesis, Properties and Applications, World Scientific Publishing Co. Pte. td. 2008.
21. Köseo?lu Y., Aldemir I., Fatih Bayansal F., Kahramanb S., Çetinkara H., Synthesis, characterization and humidity sensing properties of Mn0.2Ni0.8Fe2O4 Nanoparticles, *Mater. Chem. Phys*. 2013; **139**: 789-793.